

Prenatal exposure to nanosized zinc oxide in rats: neurotoxicity and postnatal impaired learning and memory ability

Aim: To examine the neurotoxicity of prenatal exposure to ZnO nanoparticles on rat offspring. **Materials & methods:** Pregnant Sprague-Dawley rats were exposed to ZnO nanoparticles (NPs) by gavage. Toxicity was assessed including zinc biodistribution, cerebral histopathology, antioxidant status and learning and memory capability. **Results:** A significantly elevated concentration of zinc was detected in offspring brains. Transmission electron microscope observations showed abnormal neuron ultrastructures. Histopathologic changes such as decreased proliferation and higher apoptotic death were observed. An obvious imbalanced antioxidant status occurred in brains. Adult experimental offspring exhibited impaired learning and memory behavior in the Morris water maze test compared with control groups. **Conclusion:** These adverse effects on offspring brain may cause impaired learning and memory capabilities in adulthood, particularly in female rats.

First draft submitted: 17 November 2016; Accepted for publication: 20 January 2017;
Published online: 21 March 2017

Keywords: learning and memory • neurotoxicity • oxidative stress • prenatal exposure
• ZnO nanoparticles

Along with the rapid development of nanotechnology, nanomaterials (NMs) are rapidly becoming ubiquitous in products such as cosmetics, pharmaceuticals, sunscreens and powdered foods [1]. NMs are defined as materials composed of unbound particles or particles with at least one external dimension with a primary size between 1 and 100 nm [2]. Such particles normally possess typical nanostructure-dependent properties, including chemical, biological, mechanical and optical properties. Thus, the toxicological properties of engineered nanoparticles (NPs) may greatly differ from those of their bulk counterparts [3]. However, it should be noted that NPs are not inherently benign, and they may influence biological behaviors at the cellular, protein and even genetic levels. Consequently, the vast and increasing array of engineered NPs entering the environment and society may pres-

ent health risks to workers, consumers and researchers [4].

Zinc oxide NPs are among the NMs most widely incorporated into market goods. Due to their unique photocatalytic, electronic, optical and dermatological properties, and higher bioavailability, they have been used in sunscreens [5], semiconductors [6], baby powders, shampoos, fabric treatments for UV (ultraviolet) shielding [7] and nutritional supplements [8]. In recent years, more biomedical applications have considered ZnO NPs due to their antibacterial and anticancer properties and for drug delivery [9–11]. However, the increasing applications of ZnO NPs also increase the opportunity for human contact through various exposure routes, such as ingestion [12], inhalation [13] and skin contact [14]. Unfortunately, the safety evaluation of ZnO NPs currently lags far behind their emerging development and applications.

Feng Xiaoli¹, Wu Junrong¹,
Lai Xuan¹, Zhang Yanli¹,
Wei Limin², Liu Jia¹ & Shao
Longquan^{*1}

¹Nanfang Hospital, Southern Medical University, Guangzhou 510515, China

²School & Hospital of Stomatology, Wenzhou Medical University, Wenzhou 325027, China

*Author for correspondence:
Tel.: +86 159 892 839 21
shaolongquan@smu.edu.cn

After exposure, NPs can transfer throughout the body, deposit in target organs and further cause injurious responses, such as the generation of excessive oxidative stress [15] and cell apoptosis [16]. Importantly, recent *in vivo* studies have demonstrated that ZnO NPs may transport across the blood–brain barrier (BBB) into the brain [17] or even translocate through the olfactory nerve [18]. As interest in their potential adverse effects increases, the toxic effects of ZnO NPs have been intensively studied both *in vivo* [19,20] and *in vitro* [21–23]. At present, ZnO NPs are considered to be highly toxic, with the lowest LD50 among the various engineered metal oxide NPs [24]. Many recent reports have indicated that the mechanism of nano-ZnO toxicity involves the induction of reactive oxygen species (ROS) [25], inflammation reactions [16], intracellular release of zinc ions [26] and mitochondrial abnormalities [27], among others. Although the literature on their biological effects is rapidly increasing, the knowledge on the neurotoxicological properties of ZnO NPs is still insufficient and occasionally controversial, particularly under *in vivo* conditions.

Moreover, it should be noted that the brain may be more vulnerable to NMs when exposures to such materials occur in its developmental stage. Compared with adult brains, fetal brains are more likely influenced by blood-borne substances [28]. In an animal study performed by Yamashita *et al.* [29], pregnant BALB/c mice were injected with nanosilica particles, nano-TiO₂ and fullerene C60 intravenously through the tail vein on gestational day (GD) 16 and GD 17. The author found that nanosilica and nano-TiO₂ accumulated in the placenta and fetal brain, and further caused pregnancy complications. This finding was consistent with other reports, which also indicated that NMs may cross the placenta and cause adverse effects on the developing fetus [30,31].

In fact, reproductive and developmental toxicity has been integrated into the NM research strategy of the U.S. Environmental Protection Agency [32]. However, compared with other toxicity studies, very little is known regarding the developmental neurotoxicity of ZnO NMs. In a recent study performed by Hong *et al.* [33], the author found that oral administration of 400 mg/kg/day ZnO NPs in pregnant rats would induce an embryotoxic effect. Similar toxicity was also reported in the embryos and larvae of zebra fish when exposed to nano-ZnO for 144 h postfertilization, including a decreased hatching rate and malformation occurrence [34]. However, the potential adverse effects on postnatal development and behavior in adulthood were not evaluated in the above studies. In another *in vivo* study, subcutaneous administration of ZnO NPs to the pregnant ICR (Institute of Cancer Research) mice

could alter monoaminergic neurotransmitter concentrations in the brains of 6-week-old male offspring [35]. One major limitation of this literature is that the toxicity mechanism was not involved in the experiment. Considering the current limited understanding on the developmental neurotoxicity of ZnO NPs, further detailed investigations of their adverse effects on the offspring's brain and potential complications in adulthood are urgently required.

Compared with inhalation or skin exposure, the oral intake of NPs in food-related products has more risks for the public may be under exposure of higher dose and more frequent ingestions [36,37]. To date, people possess a higher chance of being exposed to ZnO NPs than other NPs in food industry, such as nutritional additives and food packaging [38]. For this reason, the present study exposed pregnant Sprague-Dawley (SD) rats to fully characterized commercial ZnO NPs by oral administration (500 mg/kg body weight [BW]) for 18 consecutive days. There is a possibility in ZnO NPs of gaining a direct entry into the body or entering the GI tract after their accidental release into the environment as well. The doses at which humans may get exposed to these NPs at the above-mentioned scenario are yet to be found. So we choose to work with the toxicological standard recommended by KFDA (Korea Food and Drug Administration) in an oral toxicity study [39]. Furthermore, in our recent toxicology review of ZnO NPs in 2016 [40], we summarized the presence of ZnO through the gastrointestinal absorption following oral dosing as 500 mg/kg BW, and even 1–5 g/kg BW in some studies. The highest dose of 5 g/kg BW was selected on the basis of the evaluation of Scientific Committee on Cosmetic Products and Non-Food Products on normal ZnO chemical, which indicated that the LD50 of ZnO was more than 5 g/kg and no death occurred at this dose [41]. The dose level used in the current study can be used to assess the health risks from exposure to these NPs, but more safety evaluations on NPs are still required [17].

In this study, the potential neurotoxic effects on the offspring of the female rats were assessed, including the evaluation of coefficient of tissues to BW, zinc tissue biodistribution, cellular localization of ZnO NPs, cerebral histopathology, antioxidant status in the brain and the expression of oxidative stress-related genes. Furthermore, a neurobehavioral test, the Morris water maze (MWM), was performed in 8-week-old pups to determine their memory and learning abilities in adulthood. We hope that the present study will contribute to a better understanding of the nano-related risks to the CNS and raise public concerns regarding the applications of ZnO NPs, particularly in pregnant females.

Materials & methods

NP characterization

The ZnO NPs used in this study were a type of nano-powder and purchased from Sigma-Aldrich (USA).

The primary particle size and morphology were determined using a transmission electron microscope (TEM) (JEOL, Japan). The hydrodynamic size and ζ potential of NPs in distilled water (DW) were determined using a Malvern Zetasizer Nano-ZS (Malvern Instruments Ltd, UK) according to the manufacturer's instructions. Additionally, x-ray-diffraction patterns were obtained at room temperature using a RAX-10 diffractometer (SHIGAKU, UK). The specific surface area was measured through N_2 adsorption–desorption Brunauer–Emmett–Teller adsorption analysis on a Micromeritics ASAP 2010M+ C instrument (Micromeritics Co., USA). Finally, endotoxin contamination levels were measured using an E-Toxate Kit (Sigma-Aldrich, USA).

Suspensions of ZnO NPs were prepared using saline containing 0.05% v/v Tween-80. The suspensions were sonicated for 30 min using a sonicator and mechanically vibrated for 5 min prior to administration.

Durability of ZnO NPs in acidic fluid

To evaluate the durability of ZnO NPs in biological conditions, dissolution studies of NPs *in vitro* were performed in acidic gastric fluid (AGF, pH 1.5) and under neutral conditions (pH 7.0) for comparison. AGF was prepared according to a previously described method [42], and it contained 0.2% sodium chloride, 0.32% pepsin and 0.12% hydrochloric acid. Sustaining agent (saline with 0.05% Tween 80) was chosen as the control solution. NPs at 5 mg/ml were incubated in solutions for 15, 25, 45 and 60 min, and 2, 4, 6, 12 and 24 h. After incubation, the nano-ZnO suspensions were centrifuged at 15,000 $\times g$ for 30 min, then the supernatants were collected. Inductively coupled plasma–mass spectrometry (ICP–MS; Thermo Fisher Scientific, USA) was used to determine the zinc concentration.

Animals & treatment

Pregnant SD rats (220 \pm 30 g) at GD 1 were purchased from the Animal Center of Southern Medical University (Guangzhou, China). The animals were housed in stainless steel cages in a ventilated animal room under 12 h of light/dark cycle, 23 \pm 1°C and 55–65% relative humidity. Sterilized food and DW were provided *ad libitum*. All procedures used in the experiment were performed in compliance with the regulations and guidelines of the National Ethics Committee on Animal Welfare of China. The approval number provided by the ethical committee was NFYY-2014–058.

The day after arrival (GD 2), the animals were weighed and randomly divided into two groups of ten animals each, including a control group (treated with saline containing 0.05% v/v Tween-80) and an experimental group (treated with 500 mg/kg BW ZnO NP suspension). The ZnO NP suspension and the vehicle were administered to the pregnant rats by intragastric gavage daily for 18 consecutive days (on GDs 2–19). The mortality and clinical behavior were observed every day during the 18 days.

On the last day of exposure (GD 19), the female rats were housed alone and monitored for birth each day. The first day of delivery was considered to be postnatal day (PND) 0 for the pups. On PND 2, pups from eight litters (3–4 pups per litter) were selected and sacrificed by decapitation. Different tissues were collected and weighed to calculate tissue coefficients. In addition, the brain samples were used for histopathological and ultrastructural examinations or stored at -80°C for biochemical analysis. At weaning (PND 21), one pup per litter ($n = 8$) was randomly selected, anesthetized with 40 mg/kg pentobarbital sodium and subsequently sacrificed by decapitation, as were the dams in these litters. Blood (stabilized in 0.17 mol/l K₂EDTA) was thereafter quickly collected via the abdominal vein at necropsy. Brain tissues from weaned offspring ($n = 5$, one pup per litter) were also collected, immediately frozen in liquid nitrogen and maintained at -80°C. Finally, one male and one female pup from each litter ($n = 6$) were randomly selected for behavioral testing and housed as described until adulthood (PND 60). A schematic representation of the animal protocol was provided in Figure 1.

Coefficients of tissues

On PND 2, the male pups were counted and removed from each litter (3–4 per litter, $n = 8$), weighed and sacrificed by decapitation. The hearts, livers, spleens, lungs, kidneys and brains were dissected and immediately rinsed in cold saline. After weighing the bodies and tissues, the coefficients of different tissues to BW were calculated as the ratio of tissues (wet weight, mg) to BW (g).

ICP–MS elemental analysis

To evaluate tissue biodistribution, samples from the heart, liver, spleen, lung, kidney and brain were obtained from 2-day-old pups ($n = 8$). The blood samples were collected from male weaned pups (PND 21) and the dams ($n = 8$). The zinc concentrations were quantified by ICP–MS. Briefly, collected tissues (200 mg per sample) and blood (0.1 ml per sample) were predigested in concentrated nitric acid. After add-

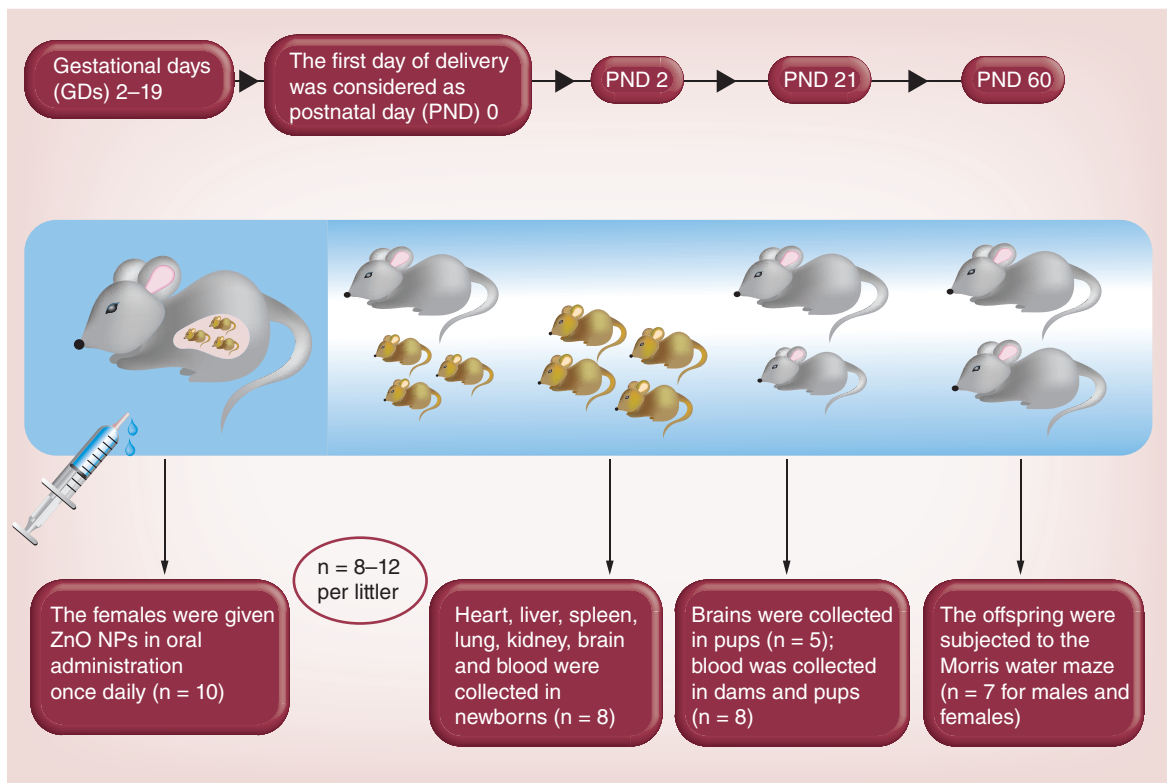


Figure 1. Schematic illustrations of experiments on the neurotoxicity of rat offspring after prenatal exposure with nano-ZnO. Pregnant rats were given nano-ZnO by gavage from GDs 2–19 once daily. The 2-day-old pups were sacrificed, and organs and blood were collected. The blood of dams and weaned pups was also collected on PND 21. The offspring were subjected to a Morris water maze to test their learning and memory ability on PND 60. GD: Gestational day; PND: Postnatal day.

ing 0.5 ml of hydrogen peroxide (H_2O_2), the mixed solutions were heated at 160°C using a high-pressure reaction container. The solutions were heated again at 120°C until the remaining nitric acid was evaporated almost to dryness. The resulting solutions were finally diluted to 2 ml with 1% nitric acid + 0.1% Triton-100 and analyzed using ICP-MS.

Histopathological examination

Brain histological analysis was performed in the male pups ($n = 5$ per group, from five different litters) on PND 2. After sacrifice, tissues were washed with 0.9% cold saline and fixed in neutral 10% buffered formalin overnight. Then, the samples were dehydrated in a series of ethanol and xylene solutions, embedded in paraffin blocks, sectioned (4 μ m) and stained with hematoxylin and eosin (H&E). Representative photos were captured using a charge-coupled device digital camera fixed to a light microscope (Olympus, Japan).

Furthermore, the presence of apoptotic and proliferating cells in brain sections was analyzed using terminal transferase-mediated dUTP (dUTPase) nick end-labeling (TUNEL) (Promega, USA) and Ki-67

immunoreactivity (Abcam, USA), respectively. The oxidative damage to nucleic acids of brain cells was analyzed by 8-hydroxy-2-deoxyguanosine (8-OhdG) immunohistochemistry (Japan Institute for the Control of Aging, Japan). Photographs of positive staining (brown) were captured at randomly selected fields both in the prefrontal cortex and hippocampus. The integrated optical density value of each image was analyzed using image proplus 6.0 software. Regions without yellow (or brown) staining served as background. All images were captured with uniform threshold and intensity settings.

TEM analysis

Brains were quickly removed from 2-day-old pups from five litters ($n = 5$) and fixed in 3% glutaraldehyde + 2% paraformaldehyde for 2 h. Small pieces of tissues (~ 1 mm 3) collected from these samples were washed with 0.1 mol/dm 3 cacodylate buffer (pH 7.2–7.4) and postfixed in 1% osmium tetroxide for 1 h. The samples were then dehydrated using a series of ethanol concentrations and embedded in Epon resin. Finally, an H-7500 TEM (Hitachi, Japan) was used to visualize the ultrathin sections (500 nm).

Biochemical parameter assay

The frozen brain samples collected from pups in PND 2 were homogenized in phosphate-buffered saline using a tissue homogenizer. The homogenate (1:9 w/v) was centrifuged at 2500 × g r.p.m. for 10 min at 4°C. After centrifugation, the supernatant was collected.

O₂⁻ in the brain tissue was measured using dichlorofluorescein-diacetate. Briefly, fresh 5% homogenate was added to a 96-well plate (190 µl per well), and then 10 µl of phosphate-buffered saline or dichlorofluorescein-diacetate working solution (dissolved in DMSO, 0.1 mmol/l) was added to each well. The plate was incubated at 37°C for 30 min in the dark. The fluorescence intensity was measured using a microplate reader (Molecular Device, USA).

Oxidative stress markers (superoxide dismutase [SOD], malondialdehyde [MDA] and glutathione peroxidase [GSH-PX]) were estimated by the Nanjing Jiancheng Bioengineering Institute (Nanjing, China) according to the manufacturer's protocols. SOD activity was determined using the xanthine oxidase method. One unit of SOD activity is the amount of SOD necessary to cause 50% inhibition of the production of nitrite. Lipid peroxidation of the brain was determined as the concentration of MDA, which could react with thiobarbituric acid reagent under acidic conditions to generate a pink-colored product. GSH-PX activities were determined following the changes in the veloc-

ity of the catalytic reaction by GSH at 37°C. Protein content was measured using Coomassie blue staining.

Total RNA extraction & real-time PCR

Brain samples were obtained from newborns (PND 2) and offspring on PND 21 (at weaning) and maintained at -80°C until analysis. Frozen tissues were homogenized and extracted using TRIzol reagent (Gibco, USA) according to the manufacturer's instructions (n = 6). The extracted RNA was further purified using Qia- gen™ RNeasy Mini columns to remove any genomic DNA contamination. The total RNA was measured at 260 and 280 nm using an M5 spectrophotometer (Molecular Devices). The purity of the RNA sample was measured as the 260/280 nm ratio with expected values between 1.8 and 2.0. Synthesized cDNA was prepared from RNA samples (1000 ng) using the PrimeScript™ RT reagent kit (TaKaRa, Japan). Real-time PCR (RT-PCR) was conducted using a commercial kit (SYBR Premix Ex Taq II, TaKaRa) and analyzed on a LightCycler 480 Sequence Detector System (Roche, Switzerland). The expression level of each target gene was normalized to its Actb mRNA content. The primers for PT-PCR are shown in Table 1.

MWM test

The MWM consisted of a large circular pool (diameter, 2.0 m) filled with water (depth, 80 cm; tempera-

Table 1. The sequence of primers used in the RT-PCR analysis.

Gene name	Description	Primer sequence	Primer size (bp)
<i>Actb</i>	Actin, beta-F	GAGAGGGAAATCGTCGTGAC	
	Actin, beta-R	CATCTGCTGGAAGGTGGACA	452
<i>SOD1</i>	Superoxide dismutase 1-F	GGTCCACGAGAAACAAGATGA	
	Superoxide dismutase 1-R	CAATCCAATCACACCACAA	101
<i>Fmo2</i>	Flavin containing monooxygenase 2-F	CCTGGAAGACTCGCTTGTAA	
	Flavin containing monooxygenase 2-R	AGGCTGGATGAGACCTATGC	112
<i>Txnip</i>	Thioredoxin interacting protein-F	TGCCCTCTGCTTGAACCTCC	
	Thioredoxin interacting protein-R	CCTACTGATTGCCACCCATC	102
<i>Gsr</i>	Glutathione reductase-F	TCCAGATGTCGATTGCCTGC	
	Glutathione reductase-R	GATCGCAACTGGGGTGAGAAA	193
<i>Keap1</i>	Kelch-like ECH-associated protein 1-F	GGGAGAGACAGCTCTGCTATT	
	Kelch-like ECH-associated protein 1-R	CAAGGGAGCAGGATGCCCTA	122
<i>Krit1</i>	KRIT1, ankyrin repeat containing-F	ATCCGACCAAAGAACACTGC	
	KRIT1, ankyrin repeat containing-R	TTCATCAGCACCACTCGTTT	242
<i>Gstt1</i>	Glutathione S-transferase theta 1-F	CAATATCCCGTTCCAGATGC	
	Glutathione S-transferase theta 1-R	CCAGGTACTCATCCACACGA	227
<i>Alox12b</i>	Arachidonate 12-lipoxygenase, 12R type-F	ACTCTCGCTGTCTGGCTTC	
	Arachidonate 12-lipoxygenase, 12R type-R	GCTTATGGCTCTCCTTGG	208

ture, 26°C), made opaque with added black ink. The pool was divided into four quadrants: northeast (NE), southeast, southwest and northwest. A circular platform (diameter, 10 cm) was placed in the middle of the NE quadrant and 2 cm below the surface of the water. Visual cues were placed on the walls surrounding the pool.

Adult rats (PND 60) received four trials a day from four starting positions with a 5-min interval. During each trial, the rats were required to find the hidden platform and spend 15 s on the platform. If they failed to find the hidden platform within 90 s, the rats were guided and placed on the platform by the experimenter and remained on it for 15 s. On the sixth day, the platform was removed from the pool and all animals were given a probe trial (60 s). Two parameters, including the number of crossings of exact position of the former platform and the swimming time in the NE quadrant (the platform location), were measured. On days 7 and 8 (reacquisition phase), reverse platform training was instituted, and the hidden platform was moved to the center of the southwest (opposite) quadrant. Reversal trials were performed as described in the acquisition phase. Throughout the training and testing, the latency to reach the platform, swim paths and the related data were recorded automatically by a video camera and a computer.

Statistical analysis

All results are expressed as the mean \pm standard error of the mean. Analysis of variance with repeated measures was applied in the MWM test. A randomized block design (one-way analysis of variance), taking into account litter effects, was used to analyze the data of coefficients of tissues. Unpaired Student's *t*-tests were applied in other comparisons between two groups. All analyses were performed in SPSS 19.0 software. A *p*-value of <0.05 was considered to be statistically significant.

Results

Physicochemical properties of ZnO NPs

The TEM micrographs demonstrated that most ZnO NPs were hexagonal with a diameter of approximately 50 nm (Figure 2A). The ZnO NPs were compared with standard crystalline zincite in the x-ray-diffraction analysis (Figure 2B). These data demonstrated that the NPs had the same crystal structure as that of the bulk zincite. The intensity-weighted average hydrodynamic diameter of the ZnO NPs in DW was 500.8 nm, which indicated that NPs formed small aggregates when dispersed in aqueous solution. In addition, the ζ potential was 32.9 mV at pH 7.0. The specific surface area of NPs was 32.17 m²/g (Table 2). The level

of endotoxin contamination was not detected (detection limit, 0.1 endotoxin units per ml). The physicochemical properties of the ZnO NPs are summarized in Table 2.

Dissolution of ZnO NPs in simulated biological fluids

The solubility data of the NPs under biological conditions are shown in Figure 3. Under neutral conditions (pH 7.0), the ZnO NPs exhibited minimal dissolution after incubation for up to 24 h (8.97 μ g/ml). However, dissociated zinc ions in the tested samples were obviously elevated under acidic conditions (pH 1.5 to mimic the gastric environment). Almost 70% of the NPs dissolved in AGF after incubation for 12 h. However, the dissolution rate subsequently slowed quickly, and the zinc concentration reached 3.53 mg/ml at 24 h. The high dissolution of ZnO NPs in the gastric environment may be taken into account when evaluating the toxicity of ZnO NPs.

Coefficients of tissues to BW

After delivery, 2-day-old pups were sacrificed, and the weights of the body and different tissues were measured (shown in Table 3). Compared with the control group, the rats in the ZnO NP-treated group had lower BWs (*p* < 0.01). Additionally, the coefficients of the brain, heart and liver in the ZnO NP-treated group were significantly higher than those in the control group (*p* < 0.05 or *p* < 0.01). In contrast, the coefficients of the kidney and spleen remarkably decreased (*p* < 0.01). Regarding the coefficients of the lung, no significant change was found in the different groups (*p* > 0.05). The different coefficient data indicate that potential injury might be induced in the pups by prenatal exposure to ZnO NPs.

Distribution pattern of zinc content

Repeated exposure to ZnO NPs for 18 days in pregnant female rats was found to result in a significant increase in the zinc concentration in various tissues of their offspring, indicating that maternal absorption and placental transfer of Zn had occurred (Figure 4). For the 2-day-old pups, Zn significantly accumulated in the heart (*p* < 0.01), liver (*p* < 0.01), kidneys (*p* < 0.01) and brain (*p* < 0.05). The maximum amount of Zn was distributed in the liver. No obvious changes in the zinc concentration were observed in the lung and spleen between the two groups (*p* > 0.05). At weaning (PND 21), however, the zinc contents in total blood were similar in the control and dams and offspring exposed to NPs (Figure 4B, *p* > 0.05), suggesting a possibility of zinc biodistribution from blood to tissues or physiological elimination of ZnO NPs from the body.

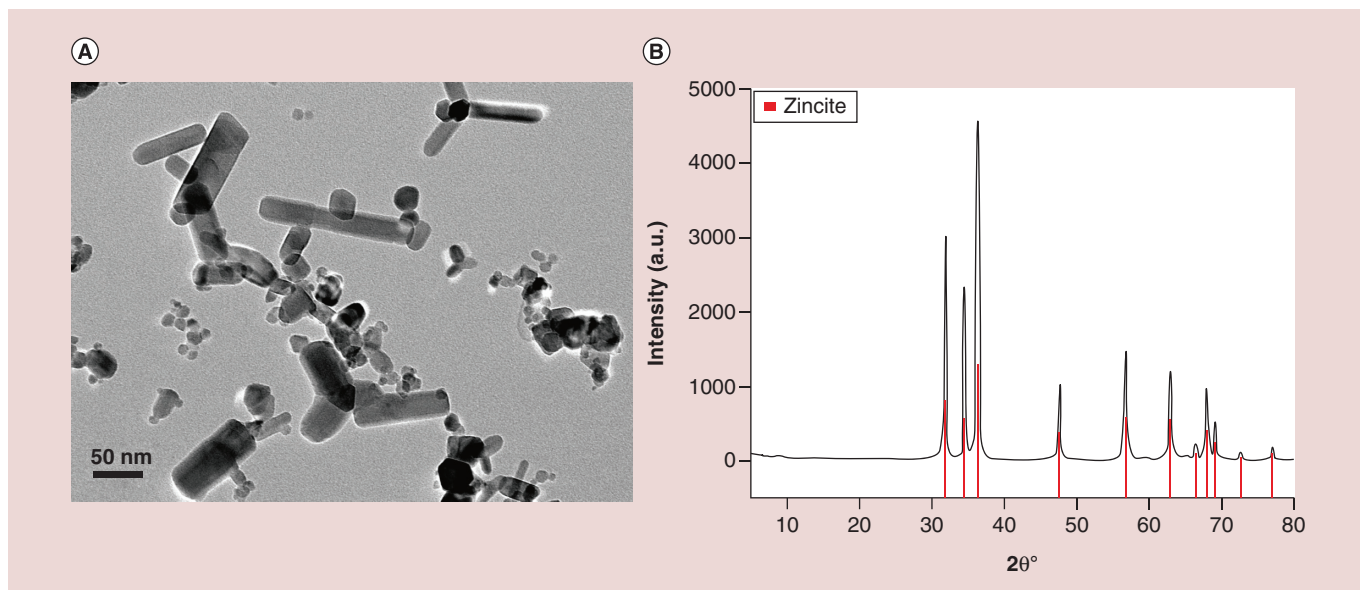


Figure 2. Particle characterization of the primary size and phase of ZnO nanoparticles. (A) TEM image of ZnO nanoparticles deposited onto a TEM grid from an ethanol solution; (B) XRD pattern of the nanoparticles (black) compared with that of the reference material zincite (red lines).

TEM: Transmission electron microscope; XRD: X-ray diffraction.

Histopathological evaluation

We examined the pathological histology of the brain in 2-day-old offspring ($n = 5$) using H&E staining (Figure 5A–H). Compared with the control offspring, the brain slices of rats prenatally treated with ZnO NPs exhibited slight abnormalities with more sparse tissue in both brain regions (Figure 5E–H). However, this change was observed in limited areas.

We further performed Ki-67 (Figure 6A–H), TUNEL (Figure 7A–H) and 8-OhdG (Figure 8A–H) immunohistochemistry to examine the effects of ZnO NPs on the proliferation and apoptotic death, and oxidative damage to nucleic acids of the brain cells. Following the administration of NPs, the number of Ki-67 positively stained (brown) cells in the prefrontal cortex and hippocampus sharply decreased (Figure 6I). Moreover, the nuclei of brain cells positively stained by TUNEL (Figure 7I) and 8-OhdG (Figure 8I) were significantly increased in both areas than that of the control pups.

Ultrastructure observation

TEM analysis revealed that the neuron in the control group contained an elliptical nucleus with homogeneous chromatin, organelles with a regular shape and

clear integrity of membranes (Figure 9A). However, the ultrastructure of the neuron from ZnO NP-exposed rats presented irregularity of the cell membrane (Figure 9B), obvious mitochondrial swelling (Figure 9C) and autophagosomes (Figure 9D). Furthermore, evidence of cellular localization of NPs was found in the neural synapse (Figure 9E & F). These results suggested that ZnO NPs accumulated in the brain cells of the pups and further induced neuron damage, which may affect normal neurofunction in adulthood.

Alteration of antioxidant status in the brain

The levels of antioxidant status in the brain are shown in Table 4. Compared with the control group, the concentrations of ROS ($p < 0.01$) and MDA ($p < 0.05$) were significantly increased in offspring exposed to ZnO NPs. Furthermore, obvious decreases in SOD ($p < 0.05$) and GSH-PX ($p < 0.01$) activities were also observed in the brains from the NP-treated group. These results suggested that prenatal exposure to ZnO NPs led to an oxidative stress situation in the brains of the offspring, which may induce oxidative damage through reactions with biomolecules such as lipids and proteins.

Table 2. Summary of physicochemical properties of ZnO nanoparticles.

Particles	Morphology	Primary size (nm)	Hydrodynamic size (nm)	ζ potential (mV)	Surface area (m ² /g)	Endotoxin (ng/ml)
ZnO	Hexagonal	50	500.8	32.9	32.17	ND
ND: Not detectable.						

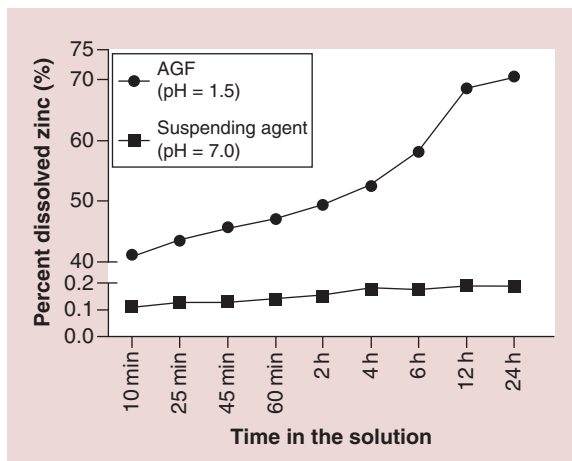


Figure 3. Dissolution of ZnO nanoparticles in the acidic gastric fluid and suspending agent at different time points.

Expression of oxidative stress-related genes

To verify the accuracy of the biochemical assays, genes associated with oxidative stress were evaluated using RT-PCR. Prenatal exposure to ZnO NPs caused subtle but significant changes in these genes in brains of newborns and weaned offspring. Of the eight genes differentially expressed in the NP exposure group, five genes were downregulated in response to the treatment (Figure 10A) at PND 2. The most differentially expressed gene in the RT-PCR analysis was SOD1, which showed the highest fold change of 0.292. In comparison, five genes were upregulated and three genes were downregulated in the brains of weaning pups (Figure 10B). Of these genes, Gstt1 and Alox12b showed higher fold changes of 3.03 and 2.853, respectively.

The effect of nano-ZnO on spatial learning & memory

The results in Figure 11 show that for all animals, the

latencies to reach the platform decreased over the course of the acquisition phase. Furthermore, on training days 1–3, there was no significant difference ($p > 0.05$) in escape latency to find the platform between the two groups. Subsequently, however, exposure to ZnO NPs exerted different effects in female and male offspring. Treatment with NPs increased the latency of female offspring to reach the platform in fourth ($p < 0.05$) and fifth ($p < 0.01$) training days. During the first day of reacquisition training, female rats in the NP group also presented longer latency to reach the platform compared with the control rats. Moreover, the NP female offspring spent less time ($p < 0.05$) in the NE quadrant (the former platform location) during the probe test (Figure 12), although the crossings over the former platform location remained unchanged ($p > 0.05$). In comparison, treatment with ZnO NPs did not alter the behavioral performance ($p > 0.05$) of nano-ZnO male offspring in the MWM.

Discussion

Nanotechnology is developing at such a rapid pace that NMs are being widely used in an extensive range of applications in different fields. Nevertheless, it should be noted that the interaction mechanisms between NPs and biological systems may be different from those of bulk materials [43]. As demonstrated in our previous review, the physicochemical properties of NPs, such as the size, shape, charge and surface modification, are important factors that mediate their interactions with cells [44]. Consequently, safety should be assessed by fully analyzing the NM and by evaluating a wide range of physical and chemical properties [45]. In our study, commercial nano-ZnO was fully characterized prior to the exposure (Table 2). Compared with inhalation or skin exposure, the oral intake of NPs in food-related products has the potential for wide public exposure

Table 3. The coefficient of tissues to body weight of 2-day-old pups.

Indexes	Group	
	ZnO NPs	Control
BW (g)	6.83 ± 0.65 [†]	7.72 ± 0.33
Heart/BW (mg/g)	6.05 ± 0.56 [†]	5.32 ± 0.42
Liver/BW (mg/g)	41.38 ± 2.77 [†]	36.66 ± 2.21
Spleen/BW (mg/g)	2.44 ± 0.42 [†]	2.82 ± 0.40
Lung/BW (mg/g)	19.60 ± 3.18	19.93 ± 1.95
Kidney/BW (mg/g)	8.66 ± 1.03 [‡]	9.28 ± 0.58
Brain/BW (mg/g)	32.77 ± 1.65 [†]	31.68 ± 1.46

[†]Significantly different from the control group at the 1% confidence level.

[‡]Significantly different from the control group at the 5% confidence level.

Values represent means ± SEM, n = 26.

BW: Body weight; NP: Nanoparticle; SEM: Standard error of the mean.

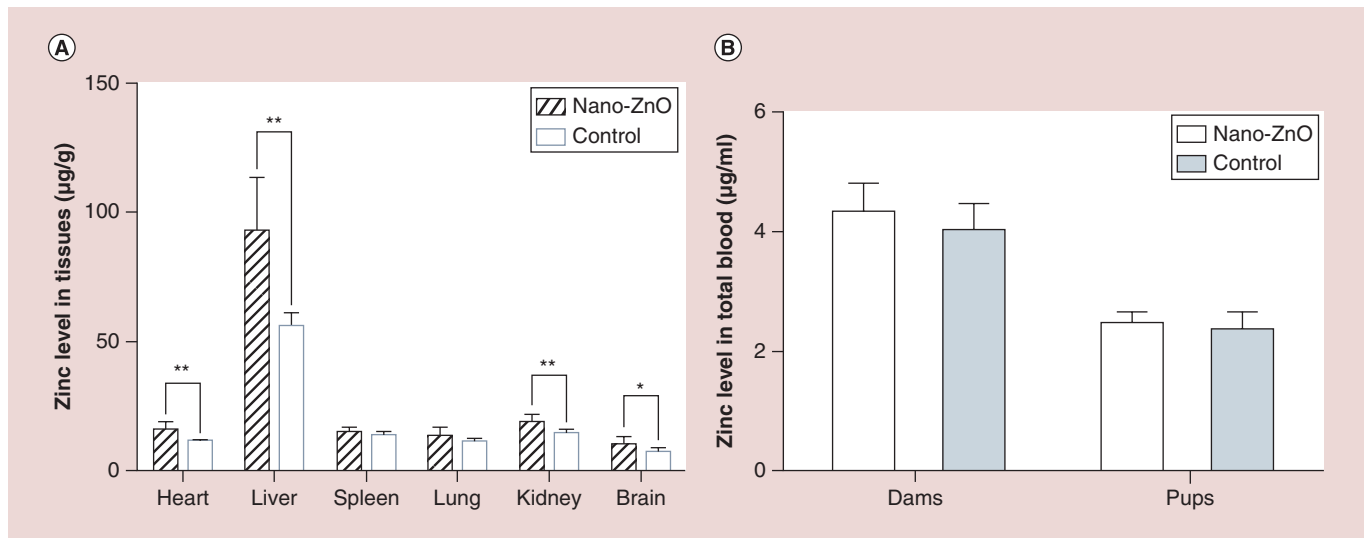


Figure 4. Zinc content in various tissues and blood evaluated by inductively coupled plasma-mass spectrometry. (A) Concentration of Zn in tissues of 2-day-old pups, including the heart, liver, spleen, lung, kidney and brain. (B) Zinc concentrations in blood of weaning pups and the dams. Data represent the mean \pm SEM, $n = 7$ for the heart, liver, spleen and brain samples, and $n = 8$ for lung, kidney and blood samples.

* $p < 0.05$; ** $p < 0.01$.

SEM: Standard error of the mean.

to higher doses and more frequent ingestion [36,37]. This study considered nano-ZnO to be a representative food-related NM and exposed pregnant SD rats to ZnO NPs by oral gavage.

Growth restriction is a common effect of chemical exposure, even when exposure occurs during the fetal stage [46]. In our study, the BWs of offspring exposed to nano-ZnO were significantly lower (Table 3) than that of the controls on PND 2. This fetal growth restric-

tion may be induced by placental dysfunction related to NP exposure [29]. It is also possible that exposure to NPs has a direct influence in fetal growth for nano-ZnO and may cross the placental barrier to reach fetal tissues [3]. In another aspect, the BW reduction might be associated with a decrease in food consumption by the pregnant dams during the treatment, which may decrease the supply of nutrients from mothers to the fetus. Regarding the coefficients of tissues, higher coef-

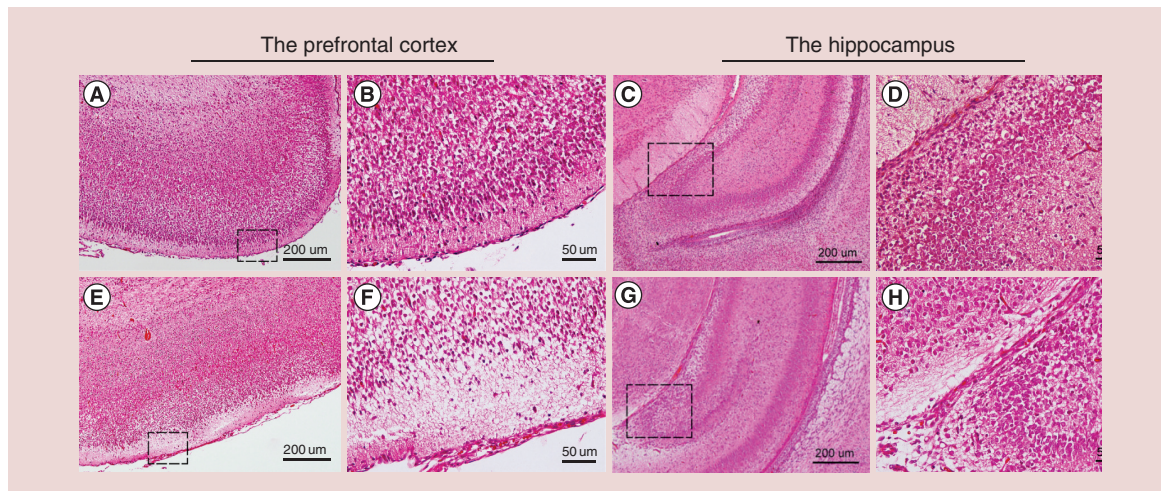


Figure 5. Pathological examination of brain tissues of the offspring. On PND 2, brain tissues from the pups in (A–D) saline-treated or (E–H) ZnO NP-treated groups were stained with H&E. (A, B, E & F) and (C, D, G & H) show the architecture of the prefrontal cortex and hippocampus, respectively. (B, D, F & H) are enlarged images of the areas within the dashed boxes in panels (A, C, E & G), respectively. Brain tissues of rats prenatally treated with ZnO NPs exhibited slight abnormalities in brain structure with more sparse tissue in both areas.

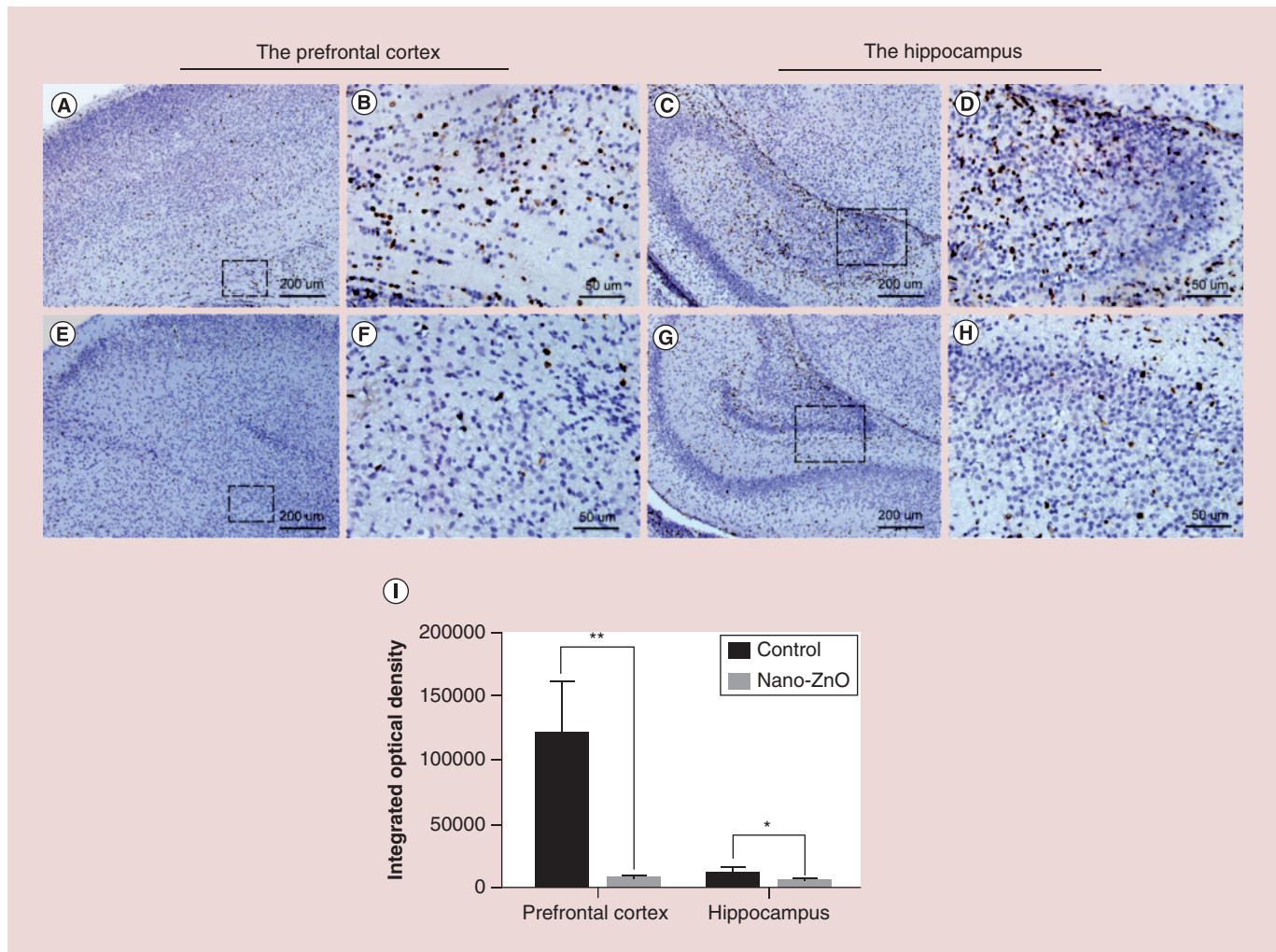


Figure 6. Ki-67 immunohistochemical analysis of brain tissues of the offspring. On PND 2, brain tissues from the pups in (A–D) saline-treated or (E–H) ZnO NP-treated groups were covered with anti-Ki-67 antibody. (A, B, E & F) and (C, D, G & H) show the architecture of the prefrontal cortex and hippocampus, respectively. (B, D, F & H) are enlarged images of the areas within the dashed boxes in (A, C, E & G), respectively. Brain tissues of rats prenatally treated with ZnO NPs exhibited smaller numbers of positively stained cells in both areas. (I) Quantitative analysis, the data represent the mean \pm SEM, $n = 5$, * $p < 0.05$, ** $p < 0.01$. This observation indicated reduced proliferation of brain cells by nano-ZnO exposure.

NP: Nanoparticle; PND: Postnatal day; SEM: Standard error of the mean.

ficients of the liver, heart and brain, and lower ratios of the spleen and kidney were observed (Table 3) in the offspring exposed to NPs. This result was highly consistent with another nano-TiO₂ toxicity study [47], even though different NMs were used in these two studies. The changing ratios of tissues to BW indicated that pathological changes, such as inflammation, might occur in the experimental offspring.

The bioavailability and toxicity of metal oxide NPs are often associated with the ability of the NPs to deliver soluble metal ions to adjacent tissues [48]. In the *in vitro* dissolution experiment, we observed that more than 70% of the NPs dissolved in AGF after incubation for 12 h (Figure 3). Several other studies showed even higher solubility of nano-ZnO in acidic envi-

ronments [42,49]. This discrepancy may be attributed to the fact that the extent of dissolution is generally dependent on particle size [50]. Furthermore, ionization of ZnO NPs in biological fluids would result in more pronounced toxicity than other NPs with longer durability under similar conditions, such as nano-TiO₂ and nano-Al₂O₃ [17,51]. Considering the acidity (pH 1.5) of the gastric fluid, a large proportion of the fed ZnO NPs may dissolve in the stomach; thus, Zn ions were absorbed into the maternal systemic circulation and further reached the fetal tissues.

In the current study, the orally administered ZnO NPs were absorbed through the GI tract and distributed to the organs of the fetus. The maximum amount of Zn was distributed in the liver, followed by the kid-

ney (Figure 4A). This result was consistent with a previous study that also observed systemic accumulations of ZnO NPs in the liver and kidney of rat offspring [52]. This biodistribution pattern may be related to the fact that the main routes of elimination of NPs are bile/liver and urine/kidney [52,53]. However, the authors found no significant differences in zinc content in the brain. In contrast, another animal study performed by Cho *et al.* [42] found elevated zinc concentrations in the brains of adult rats following oral administration. The gastric absorption of NPs is largely dependent on their size and surface properties [54,55], which may be responsible for the discrepant biodistribution patterns in different studies. Interestingly, the zinc concentrations in the blood of weaning pups and dams showed

a minimal but not statistically significant ($p > 0.05$) increase (Figure 4B). We believe that the elevated zinc concentrations in the blood might gradually decrease to a baseline because a large proportion of the NPs were distributed to organs or eliminated from the body [53].

The histopathology examination suggested that absorbed ZnO NPs posed a health risk to the offspring brain. H&E staining revealed slight and limited structural abnormalities (Figure 5). Furthermore, Ki-67 and TUNEL assays indicated that ZnO NPs might reduce proliferation (Figure 6) and induce apoptosis of brain cells (Figure 7). It is known that the hippocampus is one of the important regions of the brain that relates to learning and memory. The lesions found in this

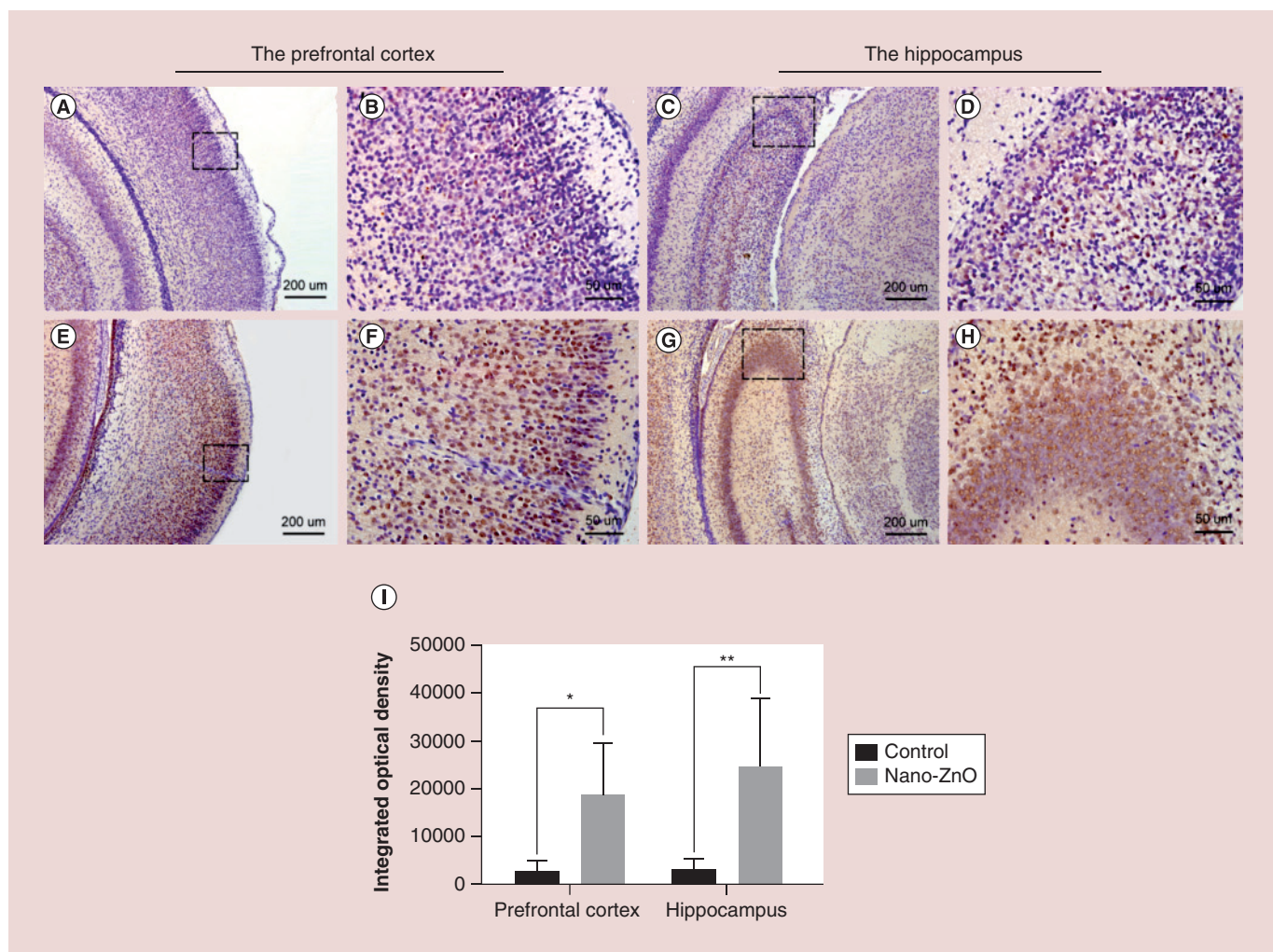


Figure 7. Transferase-mediated dUTP nick end-labeling analysis of brain tissues of the offspring. On PND 2, brain tissues from the pups in (A–D) saline-treated or (E–H) ZnO NP-treated groups were analyzed by TUNEL assay. (A, B, E & F) and (C, D, G & H) show the architecture of the prefrontal cortex and hippocampus, respectively. (B, D, F & H) are enlarged images of the areas within the dashed boxes in (A, C, E & G), respectively. Brain tissues of rats prenatally treated with ZnO NPs exhibited higher numbers of positively stained cells in both areas. (I) Quantitative analysis, data represent the mean \pm SEM, $n = 5$, * $p < 0.05$, ** $p < 0.01$. This observation indicated increased apoptosis of brain cells by nano-ZnO exposure.

NP: Nanoparticle; PND: Postnatal day; SEM: Standard error of the mean; TUNEL: Transferase-mediated dUTP nick end-labeling.

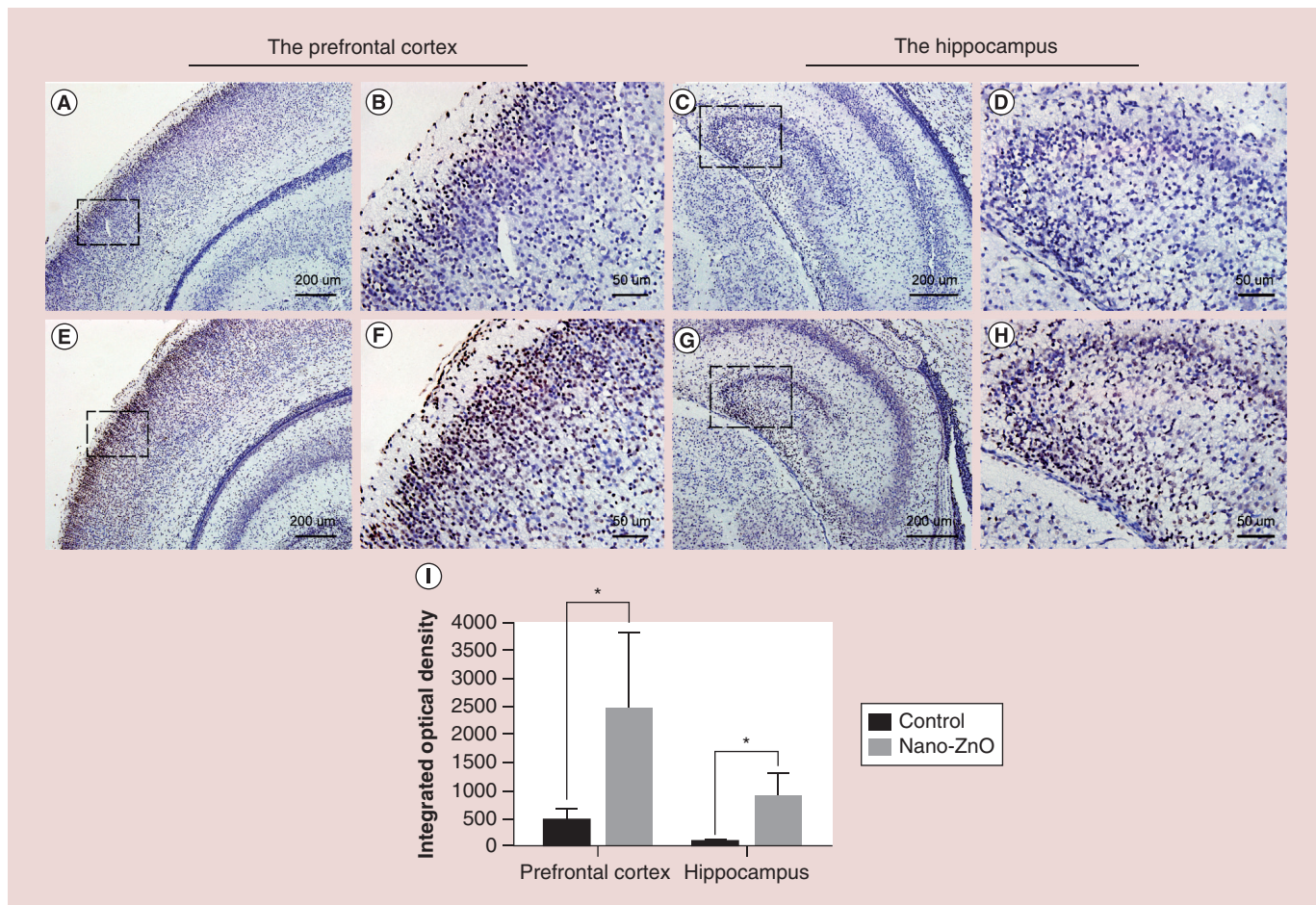


Figure 8. 8-hydroxy-2-deoxyguanosine analysis of brain tissues of the offspring. On PND 2, brain tissues from the pups in (A–D) saline-treated or (E–H) ZnO NP-treated groups were covered by anti-8-OhdG antibody. (A, B, E & F) and (C, D, G & H) show the architecture of the prefrontal cortex and hippocampus, respectively. (B, D, F & H) are enlarged images of the areas within the dashed boxes in (A, C, E & G), respectively. Brain tissues of rats prenatally treated with ZnO NPs exhibited higher numbers of positively stained cells in both areas. (I) Quantitative analysis, data represent the mean \pm SEM, $n = 5$, $*p < 0.05$. This observation indicated obvious oxidative damage to nucleic acids in the brain cells by nano-ZnO exposure.

8-OhdG: 8-Hydroxy-2-deoxyguanosine; NP: Nanoparticle; PND: Postnatal day; SEM: Standard error of the mean.

area indicated a possibility of impaired learning and memory in the adulthood.

These observed cytotoxic effects of nano-ZnO were later confirmed by TEM analysis (Figure 9). In addition to the abnormal structure of organelle, the formation of autophagosomes was found in the cytoplasm. In recent years, increasing evidence has shown that autophagy alterations may lie at the root of neurodegenerative diseases, such as Alzheimer's disease, Parkinson's disease and Huntington's disease [56,57]. Nevertheless, Roy *et al.* [58] suggested that autophagosomes may be a cellular defense mechanism against oxidative stress induced by exposure to ZnO NPs. Consequently, more evidence is required to elucidate the potential role of autophagosomes in NP-induced neuron damage. Finally, cellular accumulations of NPs were detected in the neural synapse, providing direct evidence that ZnO NPs crossed the BBB into the brain

of the fetus. Recently, several other NPs have also been reported to penetrate the BBB [59–61]. Considering the cellular localization of ZnO NPs in synapses, this finding may be associated with the possibility that NPs can be transported through nerves [18]. Accumulations of ZnO NPs in the brain cells of pups could induce neuron damage, which may affect normal brain function in their later life.

The production of free radicals has been reported for a diverse range of NMs, which may result in oxidative stress, inflammation and consequent damage to proteins, membranes and DNA [62–64]. It is known that the brain is highly vulnerable to oxidative stress because of its high metabolic rate, an inferior capacity for cellular regeneration [65]. ROS are potentially highly reactive molecules that contain an oxygen atom. An excessive production of ROS may be the initial step of oxidative stress. The overproduction of ROS

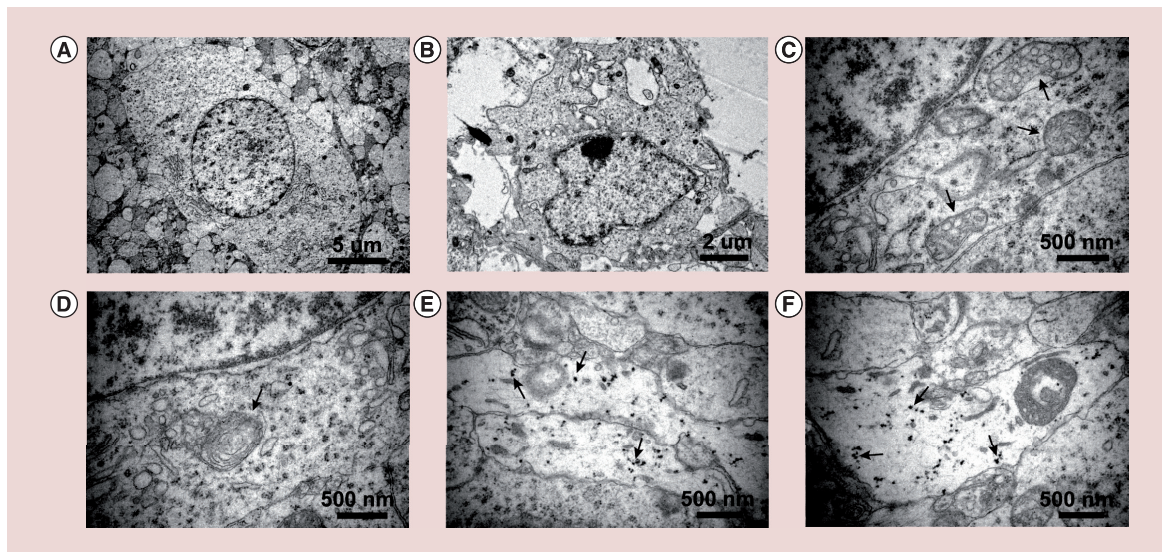


Figure 9. Ultrastructure of brain cells in 2-day-old pups. (A) Control: neuron exhibits an elliptical nucleus with homogeneous chromatin and regularly shaped organelles; (B–F) ZnO NP-treated: (B) exhibits irregularity of the cell membrane, (C) obvious mitochondrial swelling (black arrows), (D) autophagosome (black arrow), (E & F) nanoparticles (or NP aggregations) in the neural synapse (black arrows). NP: Nanoparticle.

would break down the balance of the oxidative/antioxidative system in the brain, which is closely related to the reduction of antioxidative enzymes. Inside the organism, many antioxidant enzymes, such as SOD and GSH-PX, can mitigate and repair the deleterious effects of ROS by converting superoxide ion (O_2^-) into H_2O_2 , and then into H_2O and O_2 [66,67]. In the present study, depletions in the SOD and GSH-PX levels were found in offspring exposed to ZnO NPs (Table 3). Furthermore, the content of MDA, the metabolic product of lipid peroxidation, was significantly increased compared with that in the control pups. The results of 8-OhdG immunohistochemistry (Figure 8) also revealed that NP exposure would lead to a significant oxidative damage to nucleic acids in the brain of the newborn pups. These findings indicate a generation of oxidative stress in brain tissues due to the imbalance in the ROS formation and antioxidant defense systems.

Additionally, the biochemical results were further confirmed by RT-PCR. The expression levels of genes

associated with oxidative stress revealed the differential expression of five genes in newborns and eight in weaned offspring compared with the control animals. At PND 2, five genes were downregulated in response to the treatment (Figure 10A). Of these genes, SOD1 presented the highest fold change of 0.292, followed by Gstt1 with a Diff score of 0.60. SOD1 is also known as CuZnSOD, which plays an important role in the antioxidant system by catalyzing the conversion of superoxide radicals to H_2O_2 and molecular oxygen [34]. Gstt1 is a subunit of glutathione S-transferase and metabolizes various endogenous substrates, including drugs and toxins. Therefore, decreased expression of the two genes might impair brain cell redox homeostasis through exposure to ZnO NPs.

In comparison, five genes were upregulated and three genes were downregulated in the brains of 21-day-old pups (Figure 10B). Among these genes, Gstt1 and Alox12b exhibited the highest upregulation with fold changes of 3.03 and 2.853, respectively. Alox12b

Table 4. The status of oxidative stress in the brain of nanoparticles and control offspring.

Group	ROS (FI/mg protein)	SOD (U/mg protein)	GSH-PX (U/mg protein)	MDA (nmol/mg protein)
Control	12485.56 ± 1435.13	83.36 ± 10.41	33.77 ± 2.65	12.45 ± 2.91
NPs exposed	16559.21 ± 2141.63 [†]	68.50 ± 6.90 [†]	25.32 ± 3.25 [†]	16.62 ± 2.75 [†]

[†]Significantly different from the control group at the 1% confidence level.

[‡]Significantly different from the control group at the 5% confidence level.

Values represent means ± SEM, n = 7 for ROS and GSH-PX analyses, n = 6 for SOD and MDA analyses.

FI: Fluorescence intensity; NP: Nanoparticle; ROS: Reactive oxygen species; SOD: Superoxide dismutase.

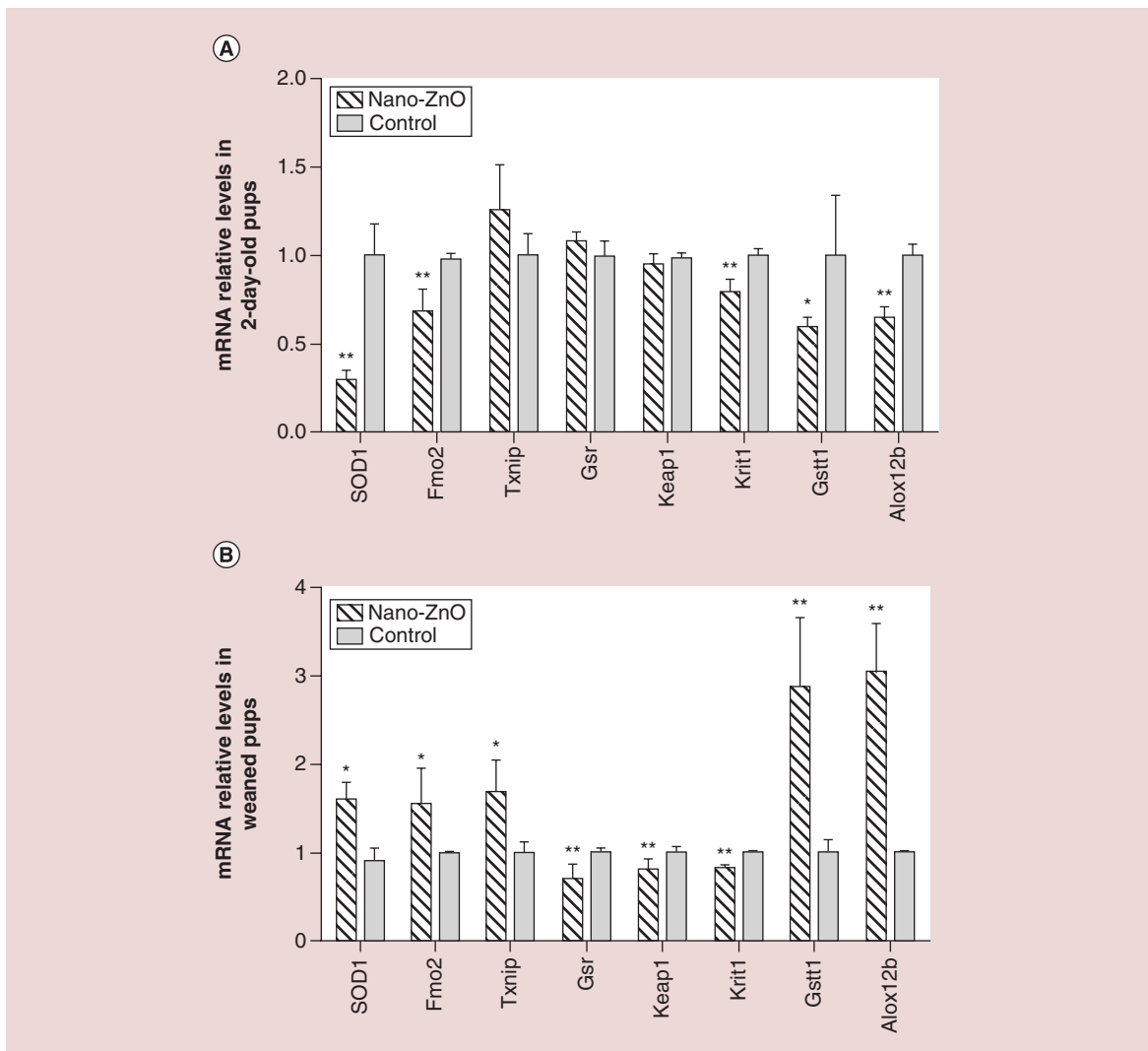


Figure 10. Expressions of oxidative stress-related genes in the offspring. (A & B) The differentially expressed genes in the brains of 2-day-old and weaned pups, respectively. Data represent the mean \pm SEM, n = 5.

*p < 0.05, **p < 0.01.

SEM: Standard error of the mean.

belongs to the LOX genes, which play a role in the oxidation-reduction process through oxidizing complex lipids and are able to modify membrane structures [68]. The upregulation of Alox12b impaired the balance of lipid oxidation, and this result was consistent with another neurotoxicity study of nano-TiO₂ [69]. Moreover, note that Gstt1 was downregulated in newborns, whereas this gene was upregulated in 21-day-old pups. This observation indicated that the expression level of the same gene may be changed during the perinatal period. We also found that more number of genes presented a response to oxidative stress in the later stage of brain development [70].

Current research has indicated that the environment that the fetus indirectly senses through the mother can be associated with other diseases in adulthood [71].

Compared with male offspring, female rats exhibited higher susceptibility to prenatal exposure to ZnO NPs, with inferior behavior performances in the water maze test. The prolonged escape latency of female offspring in the acquisition phase suggested a slowing of learning ability (Figure 11A). In addition, a decreased percentage of time in the target (NE) quadrant in which the platform was previously located showed a 'misleading' status and deteriorated memory in ZnO NP-exposed rats. Finally, NP-treated females spent a longer period of time searching the new place of the hidden platform as they tended to swim in the quadrant where the platform was originally located in the first 5 training days (Figure 12). This result implied that a former memory delayed the escape latency of the NP-exposed offspring in the reacquisition training rather than a poor

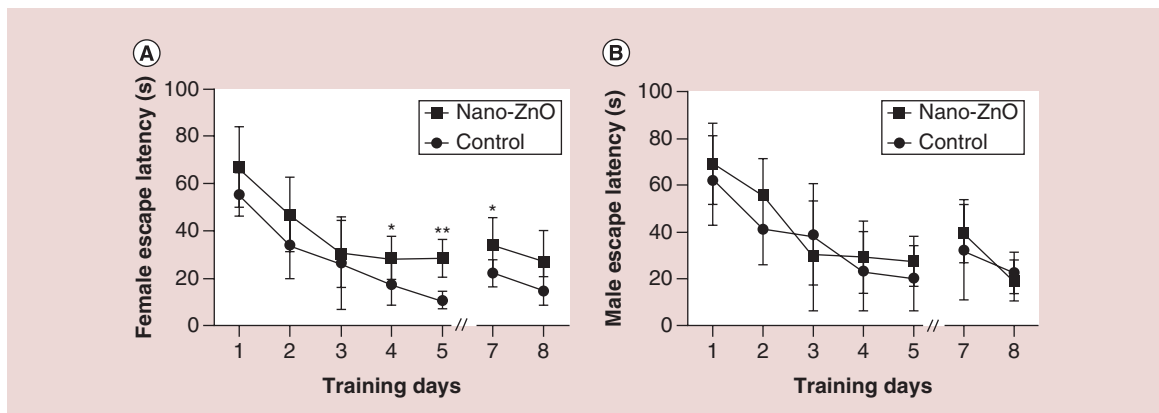


Figure 11. Escape latency to reach the platform of the Morris water maze. Animals received 5 days of training (four trials per day). On day 7, the platform was moved to a new location in the pool. The performance of (A) female offspring and (B) male offspring. Data represent the mean \pm SEM, $n = 7$ for each group.

* $p < 0.05$, ** $p < 0.01$.

SEM: Standard error of the mean.

memory. Our finding was consistent with a nano-ZnO study performed on Wistar rats using intraperitoneal administration [72].

In the current study, we think it is necessary to discriminate the neurobehavioral data between the genders because of the different motor abilities between males and females. In order to avoid the interference of native differences, we divide animals into two groups (male and female), and the comparisons were made between the same gender. According to a previous study, the performance in the reversal MWM test was linked to the ability for cognitive flexibility [73]. In the present study, the capacity to inhibit a previously obtained spatial navigation strategy and develop a new strategy simultaneously were weakened in NP-exposed female offspring. In contrast, the observation of male offspring suggested that their spatial working memory was marginally affected in comparison with the control group (Figures 11B & 12). Amara *et al.* [19] also reported

similar behavior performances of ZnO-treated male rats in the MWM test. This differential performance between male and female offspring indicated that the developmental neurotoxicity effect of ZnO NPs may be affected by sex differences. However, note that the development of the brain following prenatal exposure to ZnO NPs is not fully understood, and current contradictory investigations have been reported. Further studies are necessary to confirm this phenomenon.

Conclusion

In the present study, prenatal exposure to ZnO NPs restricted the growth of fetuses in pregnant rats. We also observed a high dissolution of NPs in AGF and obvious zinc accumulation in various organs of the offspring. Histopathology evaluation of the brain indicated slight pathological changes, including decreased proliferation and higher apoptotic death of brain cells. The neurotoxic effect of nano-ZnO was further confirmed by the

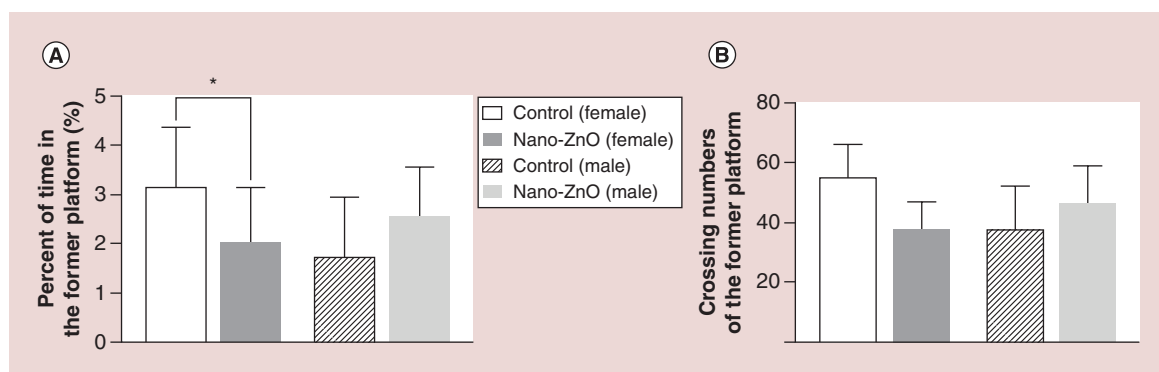


Figure 12. Probe trial performance for female and male offspring. (A) The percent of time spent in the quadrant of the former platform position. (B) Number of crossings over the former platform location. Data represent the mean \pm SEM, $n = 7$ for each group.

* $p < 0.05$.

SEM: Standard error of the mean.

abnormal ultrastructure of the neurons. Furthermore, NP-treated female offspring exhibited impaired learning and memory behavior in the MWM test in their adulthood. These structural and functional damages may be attributed to a long-term imbalanced antioxidant status in the brain tissue. However, more thorough investigations regarding the neurotoxicity of prenatal exposure to ZnO NPs are warranted. Overall, we hope that the present study will help us understand the developmental neurotoxicity of ZnO NPs and draw more attention to the safe use of NPs in pregnant females.

Financial & competing interests disclosure

This work was supported by the National Natural Science Foundation of China (81550011), Natural Science Foundation of Guang-dong Province of China (2015A030313299),

the Zhejiang Provincial Natural Science Foundation of China (LY16H140003) and the Wenzhou Municipal Science and Technology Bureau Foundation of China (Y20150070). The authors have no other relevant affiliations or financial involvement with any organization or entity with a financial interest in or financial conflict with the subject matter or materials discussed in the manuscript apart from those disclosed.

No writing assistance was utilized in the production of this manuscript.

Ethics approval and consent to participate

All animal experiments were performed in compliance with the regulations and guidelines of the National Ethics Committee on Animal Welfare of China. The approval number provided by the ethical committee of Southern Medical University was NFYY-2014-058.

Executive summary

Background

- ZnO nanoparticles (NPs) are among the engineered nanomaterials most widely incorporated into market goods. The vast and increasing applications of ZnO NPs present potential health risks to both environment and society.
- To date, knowledge on the developmental neurotoxicity of ZnO NPs remains very limited. The information is often controversial in different reports, particularly under *in vivo* conditions. It is crucial to understand the adverse effect of prenatal exposure to ZnO NPs.

Materials & methods

- Pregnant Sprague-Dawley rats were exposed to well-characterized ZnO NPs by gavage on gestational days 2–19.
- Toxicity was assessed by evaluating the tissue biodistribution and cellular localization of NPs, cerebral histopathology, antioxidant status in the brain and the expression of oxidative stress-related genes. Morris water maze was performed in 8-week-old pups to determine the learning and memory capabilities in adulthood.

Results & discussion

- Prenatal exposure to ZnO NPs was found to result in a significant increase in the zinc concentration in the brain and other tissues of rat offspring, indicating that maternal absorption and placental transfer of Zn had occurred.
- Histopathologic changes such as decreased proliferation and higher apoptotic death of the brain cells were observed in 2-day-old pups.
- Transmission electron microscope observations showed abnormal neuron ultrastructures and obvious accumulation of ZnO NPs in the synapses.
- An imbalanced antioxidant status (including elevated concentrations of reactive oxygen species occurred in the brain tissue, in parallel with differentially expressed genes such as SOD1, Fmo, Gsr and Alox12b, among others).
- Compared with male offspring, female rats exhibited higher susceptibility to prenatal exposure to ZnO NPs, with inferior behavior performances in the water maze test, suggesting an impaired learning and memory capability.

Conclusion

- Oral administration of nanosized zinc oxide in pregnant Sprague-Dawley rats will induce developmental toxicity in offspring brains. Furthermore, these adverse effects may cause impaired learning and memory capabilities in adulthood, particularly in females.

References

Papers of special note have been highlighted as: • of interest;
•• of considerable interest

- 1 Contado C. Nanomaterials in consumer products: a challenging analytical problem. *Front. Chem.* 3, 48 (2015).

- 2 Bleeker EA, De Jong WH, Geertsma RE *et al.* Considerations on the EU definition of a nanomaterial: science to support policy making. *Regul. Toxicol. Pharmacol.* 65(1), 119–125 (2013).
- 3 Hougaard KS, Jackson P, Jensen KA *et al.* Effects of prenatal exposure to surface-coated nanosized titanium

- dioxide (UV-Titan). A study in mice. *Part. Fibre Toxicol.* 7, 16 (2010).
- **Size-dependent toxicological properties of engineered nanoparticles (NPs).**
 - 4 Schug TT, Nadadur SS, Johnson AF. Nano GO Consortium – a team science approach to assess engineered nanomaterials: reliable assays and methods. *Environ. Health Perspect.* 121(6), A176–A177 (2013).
 - 5 Osmond MJ, McCall MJ. Zinc oxide nanoparticles in modern sunscreens: an analysis of potential exposure and hazard. *Nanotoxicology* 4(1), 15–41 (2010).
 - 6 Chuang HC, Juan HT, Chang CN *et al.* Cardiopulmonary toxicity of pulmonary exposure to occupationally relevant zinc oxide nanoparticles. *Nanotoxicology* 8(6), 593–604 (2014).
 - 7 Burnett ME, Wang SQ. Current sunscreen controversies: a critical review. *Photodermatol. Photoimmunol. Photomed.* 27(2), 58–67 (2011).
 - 8 Wiking L, Larsen T, Sehested J. Transfer of dietary zinc and fat to milk – evaluation of milk fat quality, milk fat precursors, and mastitis indicators. *J. Dairy Sci.* 91(4), 1544–1551 (2008).
 - 9 Niu LN, Fang M, Jiao K *et al.* Tetrapod-like zinc oxide whisker enhancement of resin composite. *J. Dent. Res.* 89(7), 746–750 (2010).
 - 10 Kasraei S, Sami L, Hendi S, Alikhani MY, Rezaei-Soufi L, Khamverdi Z. Antibacterial properties of composite resins incorporating silver and zinc oxide nanoparticles on *Streptococcus mutans* and *Lactobacillus*. *Restor. Dent. Endod.* 39(2), 109–114 (2014).
 - 11 Zhang H, Chen B, Jiang H, Wang C, Wang H, Wang X. A strategy for ZnO nanorod mediated multi-mode cancer treatment. *Biomaterials* 32(7), 1906–1914 (2011).
 - 12 Feng X, Chen A, Zhang Y, Wang J, Shao L, Wei L. Application of dental nanomaterials: potential toxicity to the central nervous system. *Int. J. Nanomedicine* 10, 3547–3565 (2015).
 - 13 Horie M, Stowe M, Tabei M, Kuroda E. Pharyngeal aspiration of metal oxide nanoparticles showed potential of allergy aggravation effect to inhaled ovalbumin. *Inhal. Toxicol.* 27(3), 181–190 (2015).
 - 14 Huang X, Wang X, Wang S, Yang J, Zhong L, Pan J. UV and dark-triggered repetitive release and encapsulation of benzophenone-3 from biocompatible ZnO nanoparticles potential for skin protection. *Nanoscale* 5(12), 5596–5601 (2013).
 - 15 Dubey A, Goswami M, Yadav K, Chaudhary D. Oxidative stress and nano-toxicity induced by TiO₂ and ZnO on WAG cell line. *PLoS ONE* 10(5), e0127493 (2015).
 - **Oxidative stress induced NP toxicity.**
 - 16 Saptarshi SR, Duschl A, Lopata AL. Biological reactivity of zinc oxide nanoparticles with mammalian test systems: an overview. *Nanomedicine* 10(13), 2075–2092 (2015).
 - 17 Shrivastava R, Raza S, Yadav A, Kushwaha P, Flora SJ. Effects of sub-acute exposure to TiO₂, ZnO and Al₂O₃ nanoparticles on oxidative stress and histological changes in mouse liver and brain. *Drug Chem. Toxicol.* 37(3), 336–347 (2014).
 - 18 Kao YY, Cheng TJ, Yang DM, Wang CT, Chiung YM, Liu PS. Demonstration of an olfactory bulb–brain translocation pathway for ZnO nanoparticles in rodent cells *in vitro* and *in vivo*. *J. Mol. Neurosci.* 48(2), 464–471 (2012).
 - 19 Amara S, Ben-Slama I, Mrad I, Rihane N, Jeljeli M, El-Mir L *et al.* Acute exposure to zinc oxide nanoparticles does not affect the cognitive capacity and neurotransmitters levels in adult rats. *Nanotoxicology* 8(Suppl. 1), 208–215 (2014).
 - 20 Shim KH, Jeong KH, Bae SO *et al.* Assessment of ZnO and SiO₂ nanoparticle permeability through and toxicity to the blood–brain barrier using Evans blue and TEM. *Int. J. Nanomedicine* 9, 225–233 (2014).
 - 21 Deng X, Luan Q, Chen W *et al.* Nanosized zinc oxide particles induce neural stem cell apoptosis. *Nanotechnology* 20(11), 115101 (2009).
 - 22 Valdiglesias V, Costa C, Kilic G *et al.* Neuronal cytotoxicity and genotoxicity induced by zinc oxide nanoparticles. *Environ. Int.* 55, 92–100 (2013).
 - 23 Sruthi S, Mohanan PV. Investigation on cellular interactions of astrocytes with zinc oxide nanoparticles using rat C6 cell lines. *Colloids Surf. B, Biointerfaces* 133, 1–11 (2015).
 - 24 Hu X, Cook S, Wang P, Hwang HM. *In vitro* evaluation of cytotoxicity of engineered metal oxide nanoparticles. *Sci. Total Environ.* 407(8), 3070–3072 (2009).
 - 25 Lu S, Zhang W, Zhang R *et al.* Comparison of cellular toxicity caused by ambient ultrafine particles and engineered metal oxide nanoparticles. *Part. Fibre Toxicol.* 12, 5 (2015).
 - 26 Wang B, Zhang YY, Mao ZW, Yu DH, Gao CY. Toxicity of ZnO nanoparticles to macrophages due to cell uptake and intracellular release of zinc ions. *J. Nanosci. Nanotechnol.* 14(8), 5688–5696 (2014).
 - 27 George S, Xia TA, Rallo R *et al.* Use of a high-throughput screening approach coupled with *in vivo* zebrafish embryo screening to develop hazard ranking for engineered nanomaterials. *ACS Nano* 5(3), 1805–1817 (2011).
 - 28 Watson RE, Desesso JM, Hurtt ME, Cappon GD. Postnatal growth and morphological development of the brain: a species comparison. *Birth Defects Res. B: Dev. Reprod. Toxicol.* 77(5), 471–484 (2006).
 - **More susceptibility of fetal brains to blood-borne substances.**
 - 29 Yamashita K, Yoshioka Y, Higashisaka K *et al.* Silica and titanium dioxide nanoparticles cause pregnancy complications in mice. *Nat. Nanotechnol.* 6(5), 321–328 (2011).
 - 30 Ghaderi S, Tabatabaei SR, Varzi HN, Rashno M. Induced adverse effects of prenatal exposure to silver nanoparticles on neurobehavioral development of offspring of mice. *J. Toxicol. Sci.* 40(2), 263–275 (2015).
 - 31 Davis DA, Bortolato M, Godar SC *et al.* Prenatal exposure to urban air nanoparticles in mice causes altered neuronal differentiation and depression-like responses. *PLoS ONE* 8(5), e64128 (2013).
 - 32 Nanomaterials Research Strategy. US Environmental Protection Agency, Washington, DC, USA, EPA 620/K-09/011 (2009). <https://nepis.epa.gov>

- 33 Hong JS, Park MK, Kim MS *et al.* Prenatal development toxicity study of zinc oxide nanoparticles in rats. *Int. J. Nanomedicine* 9(Suppl. 2), 159–171 (2014).
- 34 Zhao X, Wang S, Wu Y, You H, Lv L. Acute ZnO nanoparticles exposure induces developmental toxicity, oxidative stress and DNA damage in embryo–larval zebrafish. *Aquat. Toxicol.* 136–137, 49–59 (2013).
- 35 Okada Y, Tachibana K, Yanagita S, Takeda K. Prenatal exposure to zinc oxide particles alters monoaminergic neurotransmitter levels in the brain of mouse offspring. *J. Toxicol. Sci.* 38(3), 363–370 (2013).
- 36 Chun AL. Will the public swallow nanofood? *Nat. Nanotechnol.* 4(12), 790–791 (2009).
- 37 Rashidi L, Khosravi-Darani K. The applications of nanotechnology in food industry. *Crit. Rev. Food Sci. Nutr.* 51(8), 723–730 (2011).
- 38 Kour H, Malik AA, Ahmad N, Wani TA, Kaul RK, Bhat A. Nanotechnology – new lifeline for food industry. *Crit. Rev. Food Sci. Nutr.* doi:10.1080/10408398.2013.802662 (2015) (Epub ahead of print).
- The applications of ZnO NPs in food industry including nutritional additives and food packaging.
- 39 *Single Dose and Repeated Dose Toxicity Studies of Manufactured Nanoparticles*. Korean Food and Drug Administration, Korea, Project No. 09152nanodok700 (2010).
- 40 Liu J, Feng X, Wei L, Chen L, Song B, Shao L. The toxicology of ion-shedding zinc oxide nanoparticles. *Crit. Rev. Toxicol.* 46(4), 348–84 (2016).
- 41 Scientific Committee on Cosmetic Products and Non-Food Products (SCCNFP). Evaluation and opinion on zinc oxide. Presented at: 24th Plenary Meeting. Brussels, Belgium, 24–25 June 2003.
- 42 Cho WS, Kang BC, Lee JK, Jeong J, Che JH, Seok SH. Comparative absorption, distribution, and excretion of titanium dioxide and zinc oxide nanoparticles after repeated oral administration. *Part. Fibre Toxicol.* 10, 9 (2013).
- 43 Oberdorster G, Oberdorster E, Oberdorster J. Nanotoxicology: an emerging discipline evolving from studies of ultrafine particles. *Environ. Health Perspect.* 113(7), 823–839 (2005).
- 44 Feng X, Chen A, Zhang Y, Wang J, Shao L, Wei L. Central nervous system toxicity of metallic nanoparticles. *Int. J. Nanomedicine* 10, 4321–4340 (2015).
- 45 U.S. Food and Drug Administration (2015). www.fda.gov
- The importance of evaluation of physical and chemical properties of NPs.
- 46 Adamcakova-Dodd A, Stebounova LV, Kim JS *et al.* Toxicity assessment of zinc oxide nanoparticles using sub-acute and sub-chronic murine inhalation models. *Part. Fibre Toxicol.* 11, 15 (2014).
- 47 Wang J, Zhou G, Chen C *et al.* Acute toxicity and biodistribution of different sized titanium dioxide particles in mice after oral administration. *Toxicol. Lett.* 168(2), 176–185 (2007).
- 48 Xia T, Kovochich M, Liang M *et al.* Comparison of the mechanism of toxicity of zinc oxide and cerium oxide nanoparticles based on dissolution and oxidative stress properties. *ACS Nano* 2(10), 2121–2134 (2008).
- 49 Wang B, Feng WY, Wang M *et al.* Acute toxicological impact of nano- and submicro-scaled zinc oxide powder on healthy adult mice. *J. Nanopart. Res.* 10(2), 263–276 (2008).
- 50 Mudunkotuwa IA, Rupasinghe T, Wu CM, Grassian VH. Dissolution of ZnO nanoparticles at circumneutral pH: a study of size effects in the presence and absence of citric acid. *Langmuir* 28(1), 396–403 (2012).
- Size-dependent dissolution of ZnO NPs in acidic environments.
- 51 Cho WS, Duffin R, Howie SE *et al.* Progressive severe lung injury by zinc oxide nanoparticles; the role of Zn²⁺ dissolution inside lysosomes. *Part. Fibre Toxicol.* 8, 27 (2011).
- 52 Jo E, Seo G, Kwon JT *et al.* Exposure to zinc oxide nanoparticles affects reproductive development and biodistribution in offspring rats. *J. Toxicol. Sci.* 38(4), 525–530 (2013).
- 53 Li CH, Shen CC, Cheng YW *et al.* Organ biodistribution, clearance, and genotoxicity of orally administered zinc oxide nanoparticles in mice. *Nanotoxicology* 6(7), 746–756 (2012).
- 54 Awaad A, Nakamura M, Ishimura K. Imaging of size-dependent uptake and identification of novel pathways in mouse Peyer's patches using fluorescent organosilica particles. *Nanomed. Nanotechnol.* 8(5), 627–636 (2012).
- 55 Xia D, Cui F, Piao H *et al.* Effect of crystal size on the *in vitro* dissolution and oral absorption of nitrendipine in rats. *Pharm. Res.* 27(9), 1965–1976 (2010).
- Possible main routes of elimination of ZnO NPs.
- 56 Shacks JJ, Roth KA, Zhang J. The autophagy-lysosomal degradation pathway: role in neurodegenerative disease and therapy. *Front. Biosci.* 13, 718–736 (2008).
- 57 Cheung ZH, Ip NY. Autophagy deregulation in neurodegenerative diseases – recent advances and future perspectives. *J. Neurochem.* 118(3), 317–325 (2011).
- 58 Roy R, Singh SK, Chauhan LK, Das M, Tripathi A, Dwivedi PD. Zinc oxide nanoparticles induce apoptosis by enhancement of autophagy via PI3K/Akt/mTOR inhibition. *Toxicol. Lett.* 227(1), 29–40 (2014).
- The relationship between autophagosomes and ZnO NP-induced oxidative stress status.
- 59 Ding H, Sagar V, Agudelo M *et al.* Enhanced blood–brain barrier transmigration using a novel transferrin embedded fluorescent magneto-liposome nanoformulation. *Nanotechnology* 25(5), 055101 (2014).
- 60 Imperatore R, Carotenuto G, Di Grazia MA *et al.* Imidazole-stabilized gold nanoparticles induce neuronal apoptosis: an *in vitro* and *in vivo* study. *J. Biomed. Mater. Res. A* 103(4), 1436–1446 (2015).
- 61 Xu L, Shao A, Zhao Y *et al.* Neurotoxicity of silver nanoparticles in rat brain after intragastric exposure. *J. Nanosci. Nanotechnol.* 15(6), 4215–4223 (2015).
- 62 Bai WL, Chen YJ, Gao A. Cross talk between poly(ADP-ribose) polymerase 1 methylation and oxidative stress

- involved in the toxic effect of anatase titanium dioxide nanoparticles. *Int. J. Nanomedicine* 10, 5561–5569 (2015).
- 63 Gustafsson A, Bergstrom U, Agren L, Osterlund L, Sandstrom T, Bucht A. Differential cellular responses in healthy mice and in mice with established airway inflammation when exposed to hematite nanoparticles. *Toxicol. Appl. Pharmacol.* 288(1), 1–11 (2015).
- 64 Figarol A, Pourchez J, Boudard D *et al.* *In vitro* toxicity of carbon nanotubes, nano-graphite and carbon black, similar impacts of acid functionalization. *Toxicol. In Vitro* 30(1 Pt B), 476–485 (2015).
- 65 Cui K, Luo X, Xu K, Ven Murthy MR. Role of oxidative stress in neurodegeneration: recent developments in assay methods for oxidative stress and nutraceutical antioxidants. *Prog. Neuropsychopharmacol. Biol. Psychiatry* 28(5), 771–799 (2004).
- 66 Guan R, Kang T, Lu F, Zhang Z, Shen H, Liu M. Cytotoxicity, oxidative stress, and genotoxicity in human hepatocyte and embryonic kidney cells exposed to ZnO nanoparticles. *Nanoscale Res. Lett.* 7(1), 602 (2012).
- 67 Valavanidis A, Vlahogianni T, Dassenakis M, Scoullos M. Molecular biomarkers of oxidative stress in aquatic organisms in relation to toxic environmental pollutants. *Ecotoxicol. Environ. saf.* 64(2), 178–189 (2006).
- 68 Krieg P, Furstenberger G. The role of lipoxygenases in epidermis. *Biochim. Biophys. Acta* 1841(3), 390–400 (2014).
- 69 Ze Y, Hu R, Wang X *et al.* Neurotoxicity and gene-expressed profile in brain-injured mice caused by exposure to titanium dioxide nanoparticles. *J. Biomed. Mater. Res. A* 102(2), 470–478 (2014).
- 70 Shimizu M, Tainaka H, Oba T, Mizuo K, Umezawa M, Takeda K. Maternal exposure to nanoparticulate titanium dioxide during the prenatal period alters gene expression related to brain development in the mouse. *Part. Fibre Toxicol.* 6, 20 (2009).
- The association of indirect environment that the fetus senses with their diseases in adulthood.
- 71 Xu G, Umezawa M, Takeda K. Early development origins of adult disease caused by malnutrition and environmental chemical substances. *J. Health Sci.* 55(1), 11–19 (2009).
- 72 Han DD, Tian YT, Zhang T, Ren GG, Yang Z. Nano-zinc oxide damages spatial cognition capability via over-enhanced long-term potentiation in hippocampus of Wistar rats. *Int. J. Nanomedicine* 6, 1453–1461 (2011).
- 73 Labrie V, Duffy S, Wang W, Barger SW, Baker GB, Roder JC. Genetic inactivation of D-amino acid oxidase enhances extinction and reversal learning in mice. *Learn. Mem.* 16(1), 28–37 (2009).
- The relationship between performance in the Morris water maze test and the ability for spatial cognitive.